Article

Hydrogen Formation from Water with Various Reducing Metals Catalyzed by In Situ-Generated Nickel Nanoparticles

Ron Shirman * and Yoel Sasson

Casali Center of Applied Chemistry, Institute of Chemistry, The Hebrew University of Jerusalem,
Jerusalem 9190401, Israel; ysasson@huji.ac.il
* Correspondence: ron.shirman@mail.huji.ac.il

Abstract: Water is a potential green source for the generation of clean elemental hydrogen without contaminants. One of the most convenient methods for hydrogen generation is based on the oxidation of different metals by water. The inspection of the catalytic activity toward hydrogen formation from water performed in this study was carried out using four different metals, namely, zinc, magnesium, iron, and manganese. The process is catalyzed by in situ-generated nickel nanoparticles. The zinc–water system was found to be the most effective and exhibited 94% conversion in 4 h. The solid phase in the latter system was characterized by PXRD and SEM techniques. Several blank tests provided a fundamental understanding of the role of each constituent within the system, and a molecular mechanism for the catalytic cycle was proposed.

Keywords: hydrogen evolution; water reduction; metals; nickel catalysis; sustainability

1. Introduction

The combustion of fossil fuels releases a multitude of pollutants, including greenhouse gases, into the atmosphere, which is the primary driver of global air pollution and climate change [1,2]. This environmental impact has spurred a global interest in alternative energy sources that can mitigate these effects. Hydrogen gas has gained significant attention as an alternative energy carrier, due to its high energy conversion efficiency and the clean nature of its combustion products [3]. However, the direct utilization of hydrogen faces significant challenges, including cost considerations, safety concerns, and transportation issues, primarily because of its low density and high risk of explosion [4,5]. To address these issues, the in situ generation of hydrogen has attracted more attention in recent years. Hydrogen can be generated using three methods: biological [6,7], electrochemical [8,9], and chemical [10,11]. The chemical method is more promising when compared to the biological and electrochemical methods, which are inefficient and costly, respectively.

The chemical approach offers advantages such as safety in handling and ease of transport. It involves utilizing various hydrogen carriers capable of efficiently releasing hydrogen under controlled conditions. Examples of substances that have been advocated for as hydrogen donors are formate salts [12–14], formic acid [15,16], metal hydrides [17,18], saturated hydrocarbons [19,20], hypophosphites [21,22], and water [23,24]. Among the various hydrogen carriers, water emerges as the most promising candidate for a hydrogen source. This distinction arises from its significant hydrogen content and its safe and eco-friendly nature. [25]. Two approaches exist for generating hydrogen from water. The first is water splitting, with one type involving a photocatalyst. While environmentally friendly, this approach suffers from high energy consumption and low efficiency, limiting its commercial feasibility [11]. Another advanced method utilizes solar-driven thermochemical redox cycles, harnessing concentrated solar radiation from sources like solar towers and parabolic dishes, achieving high solar-to-fuel energy conversion efficiency [26,27]. The second method involves reacting water with a reducing agent, typically a metal, in which

hydrogen and an oxidized material (metal) are formed (Equation (1)). Typical metals used in this reaction are alkali metals, aluminum [23,28], zinc [29] and magnesium [30].

$$\text{metal} + H_2O \rightarrow \text{oxidized metal} + H_2 \tag{1}$$
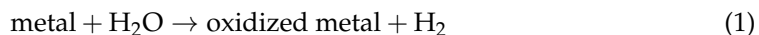
In this process, water molecules penetrate the metal cores, initiating an oxidation reaction that yields oxidized metal and pure hydrogen gas. Nevertheless, the process is not straightforward, as it involves encountering several challenges. For instance, in the case of aluminum, using an alkaline environment or milling the metal with salt have been reported as methods to address the thin oxide layer on the aluminum surface [23,31,32]. Additional challenges for other metals include the requirement to accelerate the process and to activate the metal. This is resolved by doping with additional metals, which serve as catalysts for the reaction [33]. The current trend in the transition metal catalysis process is the growing use of metals that are of lower price than platinum, palladium, and rhodium, although the noble metals are still widely used. It has been reported that nickel, separately or blended with a promoter, was found to be superior to these metals [34]. The preparation and activation of unsupported nickel catalysts have been studied by several researchers [34,35].

Herein, our research focuses on the evolution of hydrogen from the reaction between water and different metals in a neutral environment, catalyzed by in situ-generated nanoparticles of nickel. One of the key advantages of our approach is the production of a catalyst in situ, eliminating the need for prior catalyst preparation and recycling. Furthermore, unlike heterogeneous catalysts, which can suffer from decreased catalytic activity over time, our method ensures no actual damage to the catalytic activity. Additionally, we use a catalytic amount of nickel, a cost-effective alternative to expensive noble metals. Our evaluation of the metal with the highest rate of hydrogen generation among zinc, iron, magnesium, and manganese is part of our study's comprehensive comparative analysis of different metals. This unique contribution is not found in the existing literature. Additionally, we conducted targeted experiments and employed several characterization methods to clarify the role of each component in the system. This approach led to the deduction of an overall mechanism for the process. Overall, our findings contribute significantly to the development of sustainable and efficient hydrogen production methods, which are crucial for transitioning to a cleaner and greener energy landscape.

2. Materials and Methods

In a typical hydrogen generation experiment, 0.15 mol of powdered metal (9.8 g Zn, 3.6 g Mg, 8.4 g Fe, and 8.2 g Mn), 0.05 g $NiCl_2$, and 20 mL deionized water were placed in a round-bottomed flask that was connected to a reflux system in which ice water flowed, and the latter was connected to a flow-meter system that monitored the volume of hydrogen emitted (Figure 1). The reaction mixture was stirred at a rate of 1000 rpm, at 60 °C, for 24 h. The metals tested were zinc, magnesium, iron, and manganese. When the reaction was completed, the reaction mixture was centrifuged, and the solid phase was dried for 3 h at 70 °C and characterized by PXRD (X-Ray Powder Diffractometer D8 Advance, Bruker AXS, Karlsruhe, Germany) and SEM (Analytical High Resolution Scanning Electron Microscope Apreo 2S, Thermo Fisher Scientific, Waltham, MA, USA).

To assess the catalytic activity of the various systems tested, we compared their respective conversion percentages. Percentage conversion quantifies the extent to which reactants transform into products during the reaction, providing insights into catalytic efficiency. This calculation follows the formula presented in Equation (2), where $n(r)_0$ is the initial reactant mole introduced into the system and $n(r)_{end}$ is the mole of the reactant remaining at the end of the process.

$$\% \text{ Conversion} = \frac{n(r)_0 - n(r)_{end}}{n(r)_0} \times 100\% \tag{2}$$
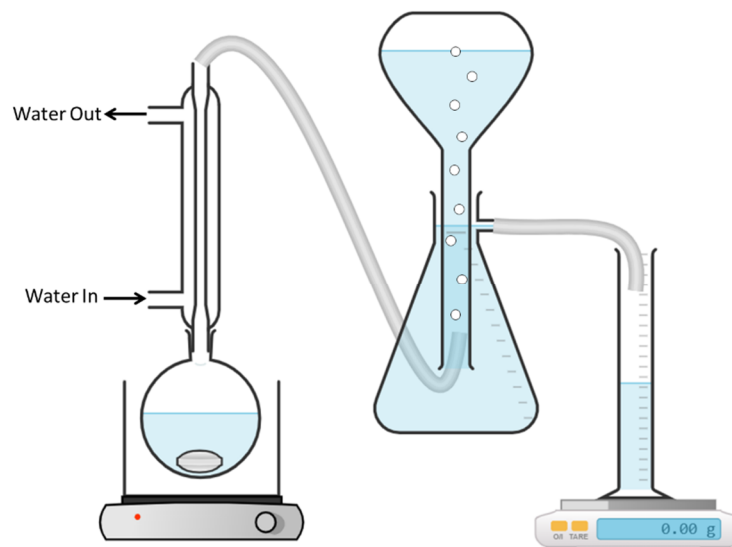
Figure 1. The flow-meter setup for monitoring the volume of hydrogen release.

3. Results and Discussion

3.1. Hydrogen Generation

Water is an excellent source of hydrogen as it is a green liquid, environmentally friendly, and abundant. The most common method currently used to produce hydrogen from water is by a water-splitting reaction (electrolysis), which uses a photocatalyst. Besides the high energy consumption of this method, very low amounts of hydrogen are obtained. For this reason, we examined the alternative way to produce hydrogen from water, that is, by reacting water with a reducing metal (Equation (1)). In this study, we followed the generation of hydrogen using different reducing metals (i.e., Zn, Mg, Fe, and Mn), and by adding nickel chloride, which turns into nickel nanoparticles that are formed in situ in the system and functions as a catalyst for the hydrogen production process. Both the metals that reduce the water and the nickel catalyst are non-noble metals. While non-noble metals may have lower resistance to oxidation and corrosion, they offer cost advantages and find widespread applications in various industries, particularly as catalysts in chemical reactions and hydrogen generation processes. The hydrogen release activity of all metal–water systems was performed under the same conditions. Figure 2 demonstrates the reaction profiles for all four systems, as determined by measuring the volume of hydrogen produced using a flow-meter system, as well as the conversions. It is apparent that the zinc–water system demonstrates remarkable activity. It reaches 94% conversion in about 4 h, while the magnesium–water system reaches 32% conversion, but the value does not stabilize even after 24 h, which means that a longer reaction time could enable the system to reach a higher % conversion. It can also be seen that the iron–water and manganese–water systems are inefficient, they reached only 8% and 14% conversion, respectively, when the reaction utterly stopped after 4 h.

In this system, the addition of nickel chloride to the system results in the in situ formation of catalytic nickel nanoparticles, which are formed by the reduction of the nickel ions by the metal. In order to examine the catalytic efficiency of the nickel nanoparticles that are formed, we performed blank experiments with and without nickel chloride. Table 1 shows the results obtained. It can be seen that the nickel particles act as a catalyst for all four systems. That is, for the zinc–water, iron–water, and manganese–water systems, no hydrogen is formed at all without the addition of nickel chloride, and for the magnesium–water system there is a 26% improvement in conversion when nickel chloride is added. For the zinc–water system, it is seen that the addition of nickel chloride causes the reaction to occur under moderate conditions and reach almost complete conversion.
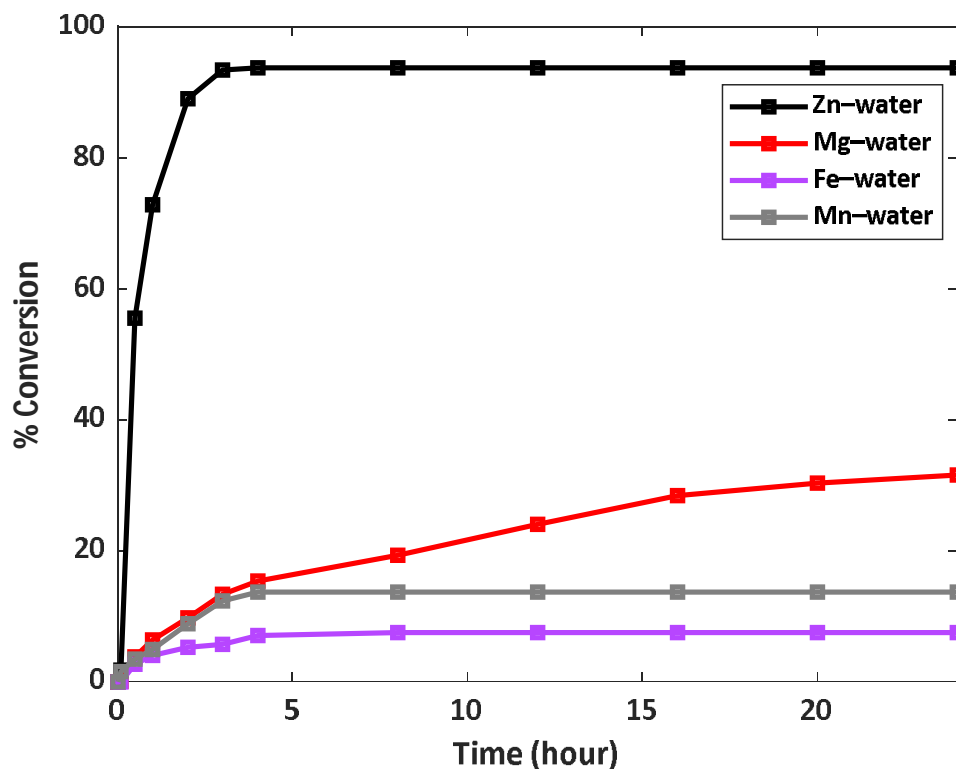
Figure 2. Kinetic profiles of the hydrogen generation from different metal–water systems at 60 °C.

Table 1. Hydrogen generation conversion with or without the addition of $NiCl_2$ to different metal–water systems at 60 °C.

Metal	% Conversion with $NiCl_2$	% Conversion without $NiCl_2$
Zn	94	0
Mg	32	6
Fe	8	0
Mn	14	0

The intrinsic catalytic activity is attributed to the diversity of metals, and, practically, this activity depends on the mass of the metal. Consequently, we investigated how variations in metal and catalyst amounts impact the conversion percentage of our most successful system, which comprises zinc, water, and nickel chloride. The results in Table 2 demonstrate the essential roles of nickel chloride and zinc in the hydrogen production reaction (entries 1 and 6). Notably, the presence of nickel significantly influences the conversion rate, with an optimal amount observed at 0.05 g, as indicated by the negligible difference between 0.05 g and 0.1 g in terms of conversion (entries 1–5). Moreover, increasing the quantity of zinc leads to a notable increase in the conversion percentage, reaching up to 94% at 9.8 g (entries 4, 6–9). However, a further increase in the zinc content to 13.1 g results in a decrease in conversion, likely due to a reduced nickel chloride to zinc ratio. This decrease in conversion could be attributed to a decrease in available chloride ions for surface cleaning of zinc, highlighting the catalytic nature of nickel chloride in the reaction.

Table 2. % Conversion of hydrogen production obtained at 60 °C for 24 h using varying masses of zinc and nickel.

Entry	m_{Zn} (g)	m_{Ni} (g)	% Conversion
1	9.8	0	0
2	9.8	0.005	54
3	9.8	0.01	90
4	9.8	0.05	94
5	9.8	0.1	95
6	0	0.05	0
7	0.3	0.05	20
8	0.7	0.05	51
9	3.2	0.05	91
10	13.1	0.05	90

3.2. Mechanistic Study

In order to determine the role of each component in the system and to appraise the molecular mechanism of the catalytic reaction, several characteristic tests of the solid phase were executed before and after the reaction for the best catalytic system. Figure 3 presents the XRD patterns of fresh zinc before the reaction and the solid phase after 24 h of the reaction. For fresh Zn, there are six peaks, at ~36.3°, ~39.02°, ~43.24°, ~54.34°, ~70.12°, and ~70.68°, which indexed with hexagonal closed pack (HCP) structure of the Zn particles. These peaks correspond to the facets (002), (100), (101), (102), (103), and (110), respectively, proving that the Zn particles are composed of pure crystalline Zn. There is a minimal percentage of zinc oxide, which is 5.2%, and, because of this, no characteristic peaks were observed. For the solid mixture collected after 24 h of reaction, it can be seen that the mixture contains 86.1% zinc hydroxide, which has four main characteristic peaks located at ~20.20°, ~20.94°, ~27.22°, and ~27.8°. These peaks correspond to the (110), (101), (111), and (201), respectively, of the crystal planes of ϵ-Zn(OH)$_2$ (Wulfingite, ICSD #50447). In addition, it can be seen that the percentage of zinc oxide has not changed, so it can be concluded that it is not created or consumed in this system.
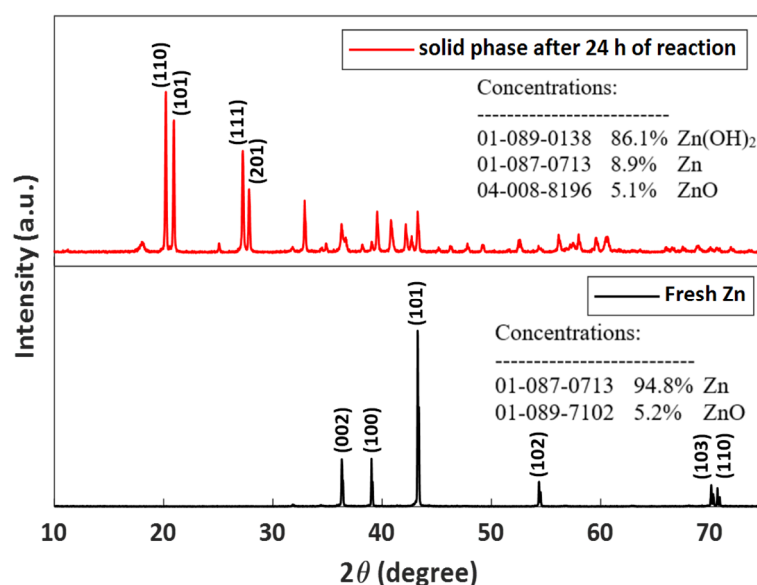

Figure 3. PXRD patterns of fresh zinc before reaction (black) and of the reaction mixture after 24 h of reaction (red).

Figure 4 shows SEM imaging of the solid phase of the reaction at three different points, i.e., fresh zinc before the reaction, after 12 h, and after 24 h. The zinc particles before the reaction have a spherical morphology with a size distribution of hundreds of nanometers

to ten microns Figure 4A-1,A-2. In the solid phase after 12 h of reaction, a change is clearly observed in the surface morphology of the particles. In Figure 4B-1 one can see that there are exposed zinc particles that did not react, and some are almost completely covered with a crystalline layer that characterizes zinc hydroxide. In the higher-resolution image, the crystalline morphology of zinc hydroxide can be seen in a more focused manner Figure 4B-2. After 24 h, the solid phase has a "broken" crystal morphology that belongs to zinc hydroxide Figure 4C-1,C-2. There is probably a small amount of zinc particles that have not reacted and were buried under the hydroxide surface.
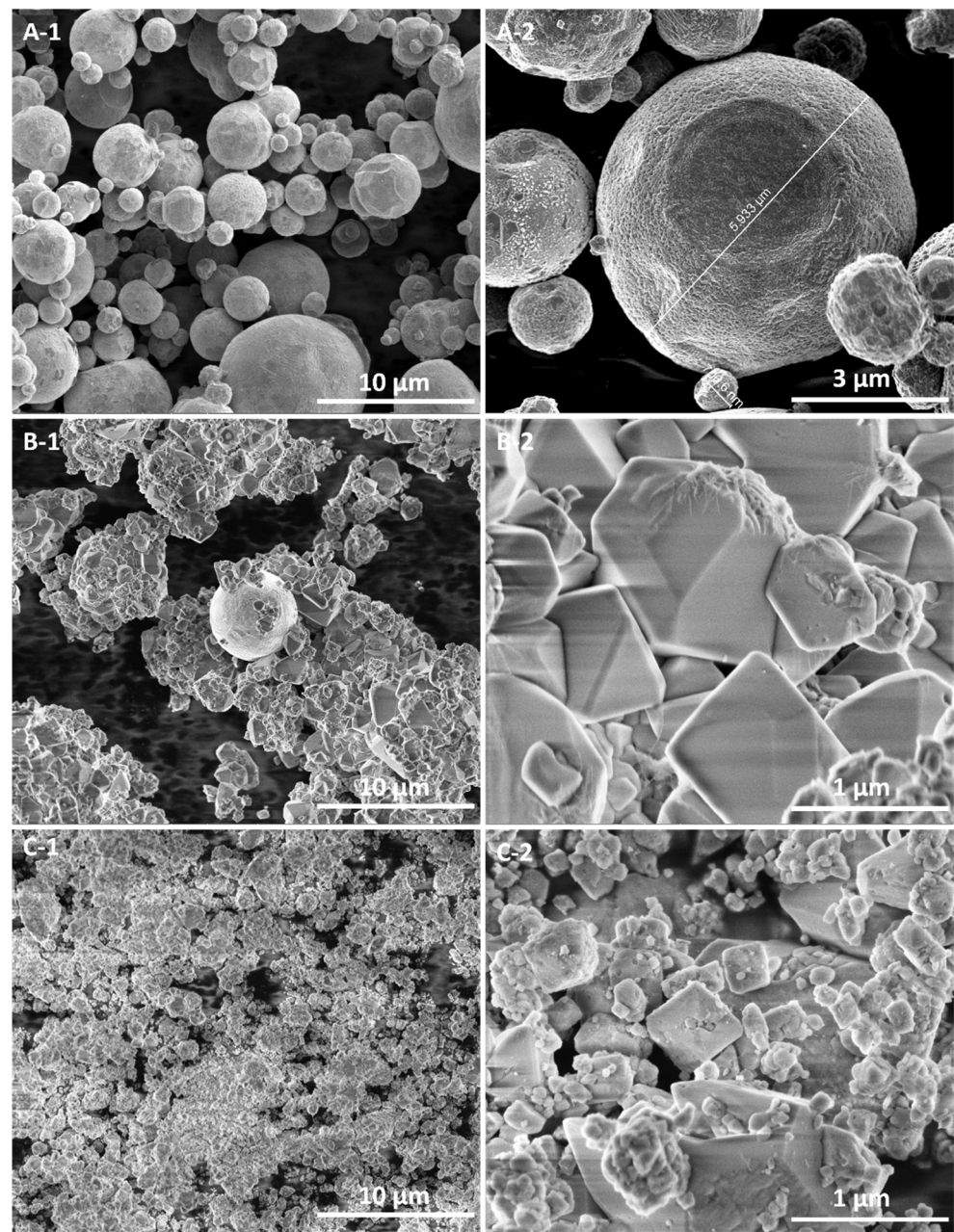

Figure 4. SEM images of (**A-1,A-2**) fresh zinc before reaction, (**B-1,B-2**) reaction mixture after 12 h of reaction, and (**C-1,C-2**) reaction mixture after 24 h of reaction.

It can be seen that the reaction manages to occur almost completely, even though zinc hydroxide is formed which blocks the surface of the zinc particles. It is assumed that the chloride ions are responsible for scrubbing the surface of the zinc particles. To verify this assumption, the activity of three systems was compared: zinc + water alone, zinc +

water + nickel chloride, and zinc + water + Raney-nickel. The system with zinc and water alone showed no reaction, while the addition of nickel chloride led to a significant 94% conversion. In contrast, using Raney-nickel, a commercial nickel catalyst devoid of chloride ions, resulted in only 31% conversion. This is substantial proof that chloride ions are indeed responsible for cleaning the hydroxide layer formed during the reaction. In order to remove the "blocked" surface after zinc hydroxide is formed a small amount of chloride is sufficient, because there is no need for complete hydroxide removal. It is enough to create tunnels in which new water molecules can seep and be adsorbed to the zinc surface. Figure 5 presents the course of action for cleaning the exterior of the zinc.
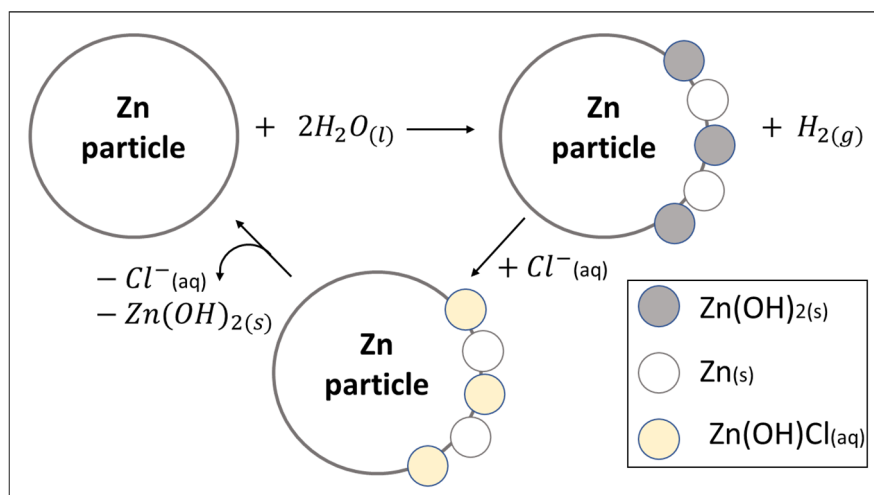

Figure 5. Cleaning process of zinc surface by chloride anion.

Figure 5 reveals that in the first step water is adsorbed on the surface of the zinc and a hydroxide layer is formed. The chloride ions present in the solution bring about an ion-exchange reaction with the hydroxide ions. A putative $Zn(OH)Cl_{(aq)}$ species is formed. This is a soluble intermediate, so this layer breaks down from the surface of the zinc. Chloride is released into the solution and can return for another round of cleaning. In the solution, the zinc ions encounter the hydroxide ions and precipitate to the bottom or/and to the surface of the zinc. This mechanism is consistent with the SEM image obtained for sample B, where one can see exposed zinc residues and areas filled with zinc hydroxide which covers the surface of the zinc particles.

For the hydrogen generation process, the stage of catalysis in the in situ formation is a reduction of nickel ions by elementary zinc (Equation (3)):

$$Zn_{(s)} + Ni^{2+}_{(aq)} \rightarrow Zn^{2+}_{(aq)} + Ni_{(s)} \tag{3}$$
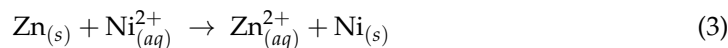
In this process, atom-sized particles of nickel are formed. We visualize that some of these are nanoparticles in solution, but, as time passes, they undergo aggregation because of the absence of any stabilizing material. This postulation also explains the plateau obtained in the hydrogen emission graph (Figure 2). It can be concluded that zinc has two functions: reducing the nickel ions to create metal nanoparticles of nickel, and producing hydrogen when it is combined with water. In fact, after the first stage, in which water molecules are adsorbed to the surface of the zinc while zinc reduces the nickel ions, metal nickel nanoparticles encounter the water molecules on the surface of the zinc and form nickel hydride (Figure 6).
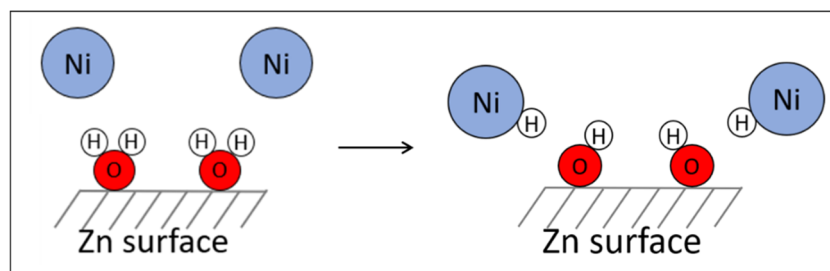
Figure 6. Generation reaction of nickel hydride.

There is chemisorption of hydrogen on the surface of the nickel. This nickel hydride exists in chemical equilibrium with metallic nickel and elementary hydrogen, where there is a transition state in which molecular hydrogen is physically adsorbed to the nickel (Equation (4)). The Ni-H species, being a transitional species, undergoes rapid decomposition into nickel and hydrogen The metallic nickel is reconstructed and can continue to release more elementary hydrogen.

$$2NiH_{(s)} \rightleftharpoons 2Ni \cdots H_2 \rightleftharpoons 2Ni_{(s)} + H_{2_{(g)}} \tag{4}$$
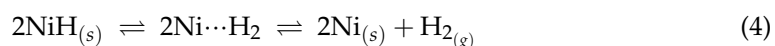
We further validated the essential role of nickel in this system by conducting experiments using other chloride-containing salts with metals capable of forming hydrides, specifically NaCl and MgCl$_2$ (Table 3). Table 3 illustrates that, despite the presence of chloride ions in sodium and magnesium chloride salts, the reaction did not proceed. Therefore, it can be inferred that nickel is indispensable in this process, and the synergistic combination of nickel and chloride is crucial for hydrogen release.

Table 3. Hydrogen generation conversion using different chloride-containing salts reacting with zinc and water at 60 °C for 24 h.

Salt	% Conversion
NaCl	3
MgCl$_2$	0.8
NiCl$_2$	94

Based on the experimental observations and characterizations, a putative catalytic cycle is herewith proposed (Figure 7). In the first step, water molecules adsorb to the surface of the zinc. At the same time, the reduction of nickel ions to metallic nickel by zinc is taking place. In the following stage, the nickel nanoparticles arrive at the surface of the zinc, where there are water molecules, and pick one hydrogen atom from each water molecule. Nickel hydride is formed. This is actually an aggregation of nickel particles, and, on some sites, there are chemisorbed hydrogen atoms on the surface of the nickel. Then, elemental hydrogen is released from the nickel hydride intermediate. Meanwhile, in order for the hydrogen generation to continue, it is important to clean parts of the zinc hydroxide layer that is formed on the zinc surface, so that additional water molecules can continue to be adsorbed. The chloride ions present in the solution perform an ion-exchange reaction with the hydroxide ions. A water-soluble species of Zn(OH)Cl$_{(aq)}$ is formed, which disintegrates from the surface of the zinc. The zinc ions meet the hydroxide ions in the solution and sediment, in part, at the bottom of the solution, and, partly, on the surface of the zinc. Chloride ions are restored and perform the cleaning process repeatedly.
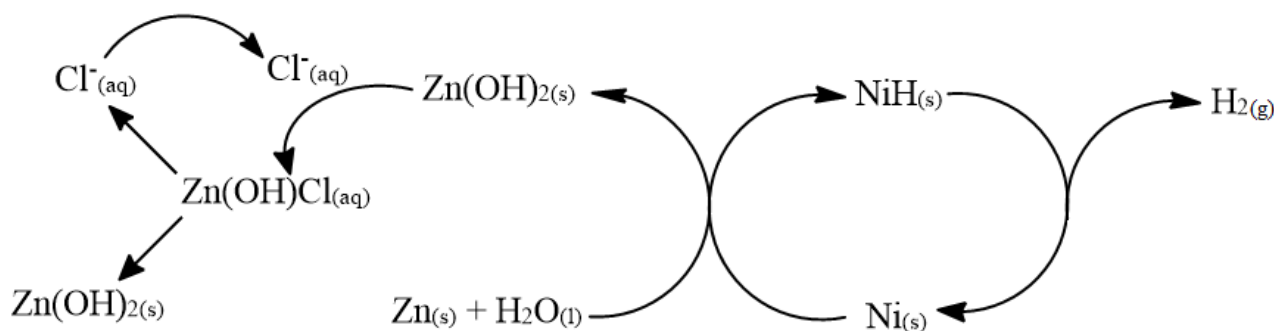
Figure 7. Catalytic mechanism of hydrogen generation from zinc–water system that is catalyzed by nickel nanoparticles formed in situ.

4. Conclusions

In conclusion, in this study, we advocate for the use of water as a source of hydrogen gas. Hydrogen generation was tested while examining the activity of four different metals as reducing agents, namely, zinc, magnesium, iron, and manganese. This process is catalyzed by in situ-generated nickel nanoparticles. The zinc–water system was found to be the most efficient for hydrogen production, which reached 94% conversion within 4 h. Based on this system, the role of each component was investigated and the catalytic mechanism for this reaction was proposed. It was found that the nickel ions were reduced in situ in the system by the metal to metallic nickel nanoparticles, which were used as a catalyst for the production of hydrogen. In this reaction, water is adsorbed to the zinc surface, nickel picks up hydrogen and releases it as elemental hydrogen, and zinc hydroxide is formed. In addition, the chloride ions play a critical role in cleaning the zinc surface in order to allow the reaction to proceed to completion. Consequently, we believe that these findings will encourage further research that will use water as a green hydrogen source combined with cheap metals under mild conditions.

References

1. Balat, M. Potential Importance of Hydrogen as a Future Solution to Environmental and Transportation Problems. *Int. J. Hydrogen Energy* **2008**, *33*, 4013–4029. [CrossRef]
2. Claxton, L.D. The History, Genotoxicity, and Carcinogenicity of Carbon-Based Fuels and Their Emissions. Part 3: Diesel and Gasoline. *Mutat. Res./Rev. Mutat. Res.* **2015**, *763*, 30–85. [CrossRef] [PubMed]
3. Deng, Z.-Y.; Ferreira, J.M.F.; Sakka, Y. Hydrogen-generation Materials for Portable Applications. *J. Am. Ceram. Soc.* **2008**, *91*, 3825–3834. [CrossRef]
4. Armaroli, N.; Balzani, V. The Hydrogen Issue. *ChemSusChem* **2011**, *4*, 21–36. [CrossRef] [PubMed]
5. San Marchi, C.; Hecht, E.S.; Ekoto, I.W.; Groth, K.M.; LaFleur, C.; Somerday, B.P.; Mukundan, R.; Rockward, T.; Keller, J.; James, C.W. Overview of the DOE Hydrogen Safety, Codes and Standards Program, Part 3: Advances in Research and Development to Enhance the Scientific Basis for Hydrogen Regulations, Codes and Standards. *Int. J. Hydrogen Energy* **2017**, *42*, 7263–7274. [CrossRef]
6. Park, W.; Hyun, S.H.; Oh, S.E.; Logan, B.E.; Kim, I.S. Removal of Headspace CO_2 Increases Biological Hydrogen Production. *Environ. Sci. Technol.* **2005**, *39*, 4416–4420. [CrossRef] [PubMed]

7. Kapdan, I.K.; Kargi, F.; Oztekin, R.; Argun, H. Bio-Hydrogen Production from Acid Hydrolyzed Wheat Starch by Photo-Fermentation Using Different *Rhodobacter* sp. *Int. J. Hydrogen Energy* **2009**, *34*, 2201–2207. [CrossRef]

8. Turner, J.; Sverdrup, G.; Mann, M.K.; Maness, P.C.; Kroposki, B.; Ghirardi, M.; Evans, R.J.; Blake, D. Renewable Hydrogen Production. *Int. J. Energy Res.* **2008**, *32*, 379–407. [CrossRef]

9. Cao, E.; Chen, Z.; Wu, H.; Yu, P.; Wang, Y.; Xiao, F.; Chen, S.; Du, S.; Xie, Y.; Wu, Y.; et al. Boron-Induced Electronic-Structure Reformation of CoP Nanoparticles Drives Enhanced PH-Universal Hydrogen Evolution. *Angew. Chem. Int. Ed.* **2020**, *59*, 4154–4160. [CrossRef]

10. Canavesio, C.; Nassini, H.E.; Bohé, A.E. Evaluation of an Iron-Chlorine Thermochemical Cycle for Hydrogen Production. *Int. J. Hydrogen Energy* **2015**, *40*, 8620–8632. [CrossRef]

11. Bahari, N.A.; Wan Isahak, W.N.R.; Masdar, M.S.; Yaakob, Z. Clean Hydrogen Generation and Storage Strategies via CO_2 Utilization into Chemicals and Fuels: A Review. *Int. J. Energy Res.* **2019**, *43*, 5128–5150. [CrossRef]

12. Zaidman, B.; Wiener, H.; Sasson, Y. Formate Salts as Chemical Carriers in Hydrogen Storage and Transportation. *Int. J. Hydrogen Energy* **1986**, *11*, 341–347. [CrossRef]

13. Horváth, H.; Papp, G.; Kovács, H.; Kathó, Á.; Joó, F. Iridium(I)–NHC-Phosphine Complex-Catalyzed Hydrogen Generation and Storage in Aqueous Formate/Bicarbonate Solutions Using a Flow Reactor—Effective Response to Changes in Hydrogen Demand. *Int. J. Hydrogen Energy* **2019**, *44*, 28527–28532. [CrossRef]

14. Shirman, R.; Bahuguna, A.; Sasson, Y. Effect of Precursor on the Hydrogen Evolution Activity and Recyclability of Pd-Supported Graphitic Carbon Nitride. *Int. J. Hydrogen Energy* **2021**, *46*, 36210–36220. [CrossRef]

15. Wang, Z.-L.; Yan, J.-M.; Ping, Y.; Wang, H.-L.; Zheng, W.-T.; Jiang, Q. An Efficient CoAuPd/C Catalyst for Hydrogen Generation from Formic Acid at Room Temperature. *Angew. Chem.* **2013**, *125*, 4502–4505. [CrossRef]

16. Wang, X.; Meng, Q.; Gao, L.; Jin, Z.; Ge, J.; Liu, C.; Xing, W. Recent Progress in Hydrogen Production from Formic Acid Decomposition. *Int. J. Hydrogen Energy* **2018**, *43*, 7055–7071. [CrossRef]

17. Sakintuna, B.; Lamari-Darkrim, F.; Hirscher, M. Metal Hydride Materials for Solid Hydrogen Storage: A Review. *Int. J. Hydrogen Energy* **2007**, *32*, 1121–1140. [CrossRef]

18. Tarasov, B.P.; Fursikov, P.V.; Volodin, A.A.; Bocharnikov, M.S.; Shimkus, Y.Y.; Kashin, A.M.; Yartys, V.A.; Chidziva, S.; Pasupathi, S.; Lototskyy, M.V. Metal Hydride Hydrogen Storage and Compression Systems for Energy Storage Technologies. *Int. J. Hydrogen Energy* **2021**, *46*, 13647–13657. [CrossRef]

19. Feng, Z.; Chen, X.; Bai, X. Catalytic Dehydrogenation of Liquid Organic Hydrogen Carrier Dodecahydro-N-Ethylcarbazole over Palladium Catalysts Supported on Different Supports. *Environ. Sci. Pollut. Res.* **2020**, *27*, 36172–36185. [CrossRef]

20. Luo, N.; Cao, F.; Zhao, X.; Xiao, T.; Fang, D. Thermodynamic Analysis of Aqueous-Reforming of Polyols for Hydrogen Generation. *Fuel* **2007**, *86*, 1727–1736. [CrossRef]

21. Shirman, R.; Sasson, Y. Hydrogen Generation from Sodium Hypophosphite Catalyzed by Metallic Nanoparticles Supported on Graphitic Carbon Nitride. *Int. J. Hydrogen Energy* **2023**, *48*, 27611–27618. [CrossRef]

22. Nikoleishvili, P.; Gorelishvili, G.; Kveselava, V.; Kurtanidze, R.; Gogoli, D.; Sharabidze, D. Hydrogen Generation from the Hydrolysis of Sodium Hypophosphite Using CoB_2O_4 Catalyst. *ECS Meet. Abstr.* **2016**, *MA2016-01*, 1555. [CrossRef]

23. Mahmoodi, K.; Alinejad, B. Enhancement of Hydrogen Generation Rate in Reaction of Aluminum with Water. *Int. J. Hydrogen Energy* **2010**, *35*, 5227–5232. [CrossRef]

24. Xie, G.; Zhang, K.; Guo, B.; Liu, Q.; Fang, L.; Gong, J.R. Graphene-Based Materials for Hydrogen Generation from Light-Driven Water Splitting. *Adv. Mater.* **2013**, *25*, 3820–3839. [CrossRef] [PubMed]

25. Tzimas, E.; Filiou, C.; Peteves, S.D.; Veyret, J.B. *Hydrogen Storage: State-of-the-Art and Future Perspective*; EU Commission: Petten, The Netherlands, 2003; pp. 1511–1519.

26. Abanades, S.; Charvin, P.; Flamant, G.; Neveu, P. Screening of Water-Splitting Thermochemical Cycles Potentially Attractive for Hydrogen Production by Concentrated Solar Energy. *Energy* **2006**, *31*, 2805–2822. [CrossRef]

27. Abanades, S. Metal Oxides Applied to Thermochemical Water-Splitting for Hydrogen Production Using Concentrated Solar Energy. *ChemEngineering* **2019**, *3*, 63. [CrossRef]

28. Gai, W.Z.; Liu, W.H.; Deng, Z.Y.; Zhou, J.G. Reaction of Al Powder with Water for Hydrogen Generation under Ambient Condition. *Int. J. Hydrogen Energy* **2012**, *37*, 13132–13140. [CrossRef]

29. Mukhopadhyay, S.; Rothenberg, G.; Wiener, H.; Sasson, Y. Solid–Solid Palladium-Catalysed Water Reduction with Zinc: Mechanisms of Hydrogen Generation and Direct Hydrogen Transfer Reactions. *New J. Chem.* **2000**, *24*, 305–308. [CrossRef]

30. Bartali, R.; Speranza, G.; Aguey-Zinsou, K.F.; Testi, M.; Micheli, V.; Canteri, R.; Fedrizzi, M.; Gottardi, G.; Coser, G.; Crema, L.; et al. Efficient Hydrogen Generation from Water Using Nanocomposite Flakes Based on Graphene and Magnesium. *Sustain. Energy Fuels* **2018**, *2*, 2516–2525. [CrossRef]

31. Parmuzina, A.V.; Kravchenko, O.V. Activation of Aluminium Metal to Evolve Hydrogen from Water. *Int. J. Hydrogen Energy* **2008**, *33*, 3073–3076. [CrossRef]

32. Rosen, M.A. Advances in Hydrogen Production by Thermochemical Water Decomposition: A Review. *Energy* **2010**, *35*, 1068–1076. [CrossRef]

33. Chen, K.F.; Li, S.; Zhang, W.X. Renewable Hydrogen Generation by Bimetallic Zero Valent Iron Nanoparticles. *Chem. Eng. J.* **2011**, *170*, 562–567. [CrossRef]

34. Tasker, S.Z.; Standley, E.A.; Jamison, T.F. Recent Advances in Nickel Catalysis. *Nature* **2014**, *509*, 299–309. [CrossRef] [PubMed]
35. Nishimura, S. *Handbook of Heterogeneous Catalytic Hydrogenation for Organic Synthesis*; John Wiley & Sons: Hoboken, NJ, USA, 2001.